Atomic ESR relaxation in tritiated solid hydrogen

G. W. Collins, J. L. Maienschein, E. R. Mapoles, R. T. Tsugawa, E. M. Fearon, and P. C. Souers
Lawrence Livermore National Laboratory, University of California, Livermore, California 94550

J. R. Gaines
Department of Physics, University of Hawaii, Honolulu, Hawaii 96822

P. A. Fedders
Department of Physics, Washington University, St. Louis, Missouri 63130
(Received 12 June 1992; revised manuscript received 1 February 1993)

Electron-spin-resonance data taken at 9 GHz for hydrogen atoms in tritiated solid H_2, HD, D_2, D-T, and T_2 are presented. Both linewidths and longitudinal relaxation times have been measured simultaneously with $J=1$ and hydrogen-atom concentrations. Data are presented to show that the line shapes can be inhomogeneous. Linewidth calculations using the weak dipolar interaction and hyperfine interaction are presented. Both predict Gaussian lines, and agreement is poor with the measured line shapes that are more often closer to Lorenzian. The Gaussian theories may be useful only for a few data points taken with high $J=1$ concentration and at high temperature. A dilute-spin theory for atom-atom interactions when little $J=1$ hydrogen is present, fails to work as well. The best line-shape agreement is obtained with a combination of $J=1$ and atom concentrations, both to the half power. D_2 fails conspicuously with every approach. The longitudinal relaxation times appear constant at 0.1–1 s except at low $J=1$ concentrations, where the relaxation times increase. The electric-quadrupole mechanism is postulated for low $J=1$ concentrations, but it does not show the expected $J=1$ dependence. No information on "hidden" atoms is forthcoming from these data, but their presence is still a possibility.

I. INTRODUCTION

The search for ever more energetic materials continues. A possible cryogenic fuel could be solid hydrogen containing hydrogen atoms, which would produce large energies of recombination upon demand. We have recently measured by 9-GHz electron spin resonance (ESR) the concentration of hydrogen atoms in solid tritium (T_2) and deuterium-tritium (D-T) and found several hundred to a few thousand parts per million.[1] However, Gaines, Cao, and Fedders have recently suggested that the ESR linewidths of atoms closely packed into bubbles could be so broadened as to render these atoms invisible.[2] A major issue in this field is whether hidden atoms contain vast energies that render solid hydrogen a viable cryogenic fuel. This information could be hidden in the relaxation properties of the visible atoms.

We here present our ESR data for linewidth and longitudinal relaxation. As a further issue, the basic question of the mechanism of atom linewidths is undecided. Sharnoff and Pound used a weak dipolar model[3] whereas Miyazaki *et al.* have recently used a hyperfine interaction model.[4,5] Another undecided issue is whether the atom linewidths are homogeneous or inhomogeneous. Finally, we present the first substantial quantity of longitudinal relaxation data, where the mechanism has not been considered.

II. EXPERIMENT

Our apparatus has been previously described.[1] We shall summarize by noting that 9.4-GHz ESR was carried out using a homodyne detector. No modulation was used, and the data presented here are known to be unsaturated, because the longitudinal relaxation times were simultaneously measured. Care was also taken to ensure that adiabatic slow passage conditions were also met. Because of the low 9-GHz frequency, we were only able to see the narrow linewidth ($\sim$10 MHz) atom species. At 24 GHz, Sharnoff and Pound observed an additional broad line ($\sim$300 MHz) species, showing that, indeed, other atoms are present.[3]

Also, most of the data listed here are for the solid without the known presence of heat spikes.[6] These heat pulses take place spontaneously at 3 K and below in the ESR cell and occur when large numbers of atoms cooperatively recombine.

It is essential to know the $J=1$-to-0 time constants for the various species. A large quantity of D-T and T_2 data have been listed previously, and both the conversion time constants and probable steady-state concentrations are known.[7] For this work, we also needed conversion data for H_2, HD, and D_2, all doped with 2 at. % tritium. The H_2 data were taken easily by observing the decay of the $J=1$ H_2 free-induction decay (FID). We measured 22 h for the $J=1$-to-0 time constants at 1.4 K and 7 h at 5.4 K; and we interpolated for the 4.0-K H_2 run. FID's could not be used for either HD or D_2, and the longitudinal relaxation times were measured. These could not be related accurately to $J=1$-to-0 conversion times, although times of 10–50 h appear likely. In HD, the initial $J=1$ concentration is only about 1% due to H_2 and D_2 impurities. In D_2, both the $J=1$ and 0 species are NMR

active so that conversion is not expected to create large changes in linewidth.

Calculated second moments from the data diverged and were not obtainable. We then sought to describe the ESR lines as a mixture of Lorentzian and Gaussian lines. If A is the area of the line, $\Delta\nu$ the linewidth, and S_m the line intensity, then we define the constants[8]

$$B(\text{Lorentzian line}) = A/S_m\Delta\nu = 1.57\ , \quad (1)$$

$$B(\text{Gaussian line}) = A/S_m\Delta\nu = 1.06\ . \quad (2)$$

This allows us to calculate the fraction of the Lorentzian line component, L, for a given measurement, B, equal to

$$L = (B-1.06)/(1.57-1.06)\ . \quad (3)$$

The electron longitudinal relaxation time T_{1e} was measured by the saturation-recovery method.[9] The microwave source was a reflex klystron with a 10-kHz spectral width and an output power of 600 nW at the peak of its mode. Pin diode switches were used to form the high-power pulses. For a T_{1e} measurement, a high-power microwave pulse of about 100 mW is applied to the sample until the spins are completely saturated. The high power was then turned off and low-power microwaves of about 1 nW were used to monitor the recovery of the spins from the saturated state back to a Boltzmann distribution. The recovery of the spins was recorded on a digital oscilloscope to allow signal averaging. The signal height at time t, S, and at time zero, $S(0)$, are related by

$$S = S(0)\exp(-t/T_{1e})\ . \quad (4)$$

TABLE I. Measured relaxation times, $J=1$ compositions, and atom densities for solid H_2 and T_2.

Hydrogen	Time (min)	Linewidth (MHz)	$J=1$ H_2 or T_2 (%)	Electron T_{1e} (ms)	Total atoms (ppm)	Hydrogen	Time (min)	Linewidth (MHz)	$J=1$ T_2 (%)	Electron T_{1e} (ms)	Total atoms (ppm)
H_2	13	3.1	74		8	T_2	95	7.8	21		201
1.4 K	33	3.4	73	476	22	4.0 K	199	8.1	6.4		238
	63	3.1	71	388	30		285	8.1	3.1	65	252
	158	3.1	66	353	55		430	7.8	2.1	64	249
	435	2.8	53	280	90		822	9.2	2.1	66	311
	1486	2.5	23	270	124		1152	9.5	2.1	69	372
	1903	2.5	17	270	135	T_2	0	6.7	65		16
	3448	2.5	5.0	438	155	5.1 K	6	6.7	62		49
	5846	2.2	0.8	784	175		11	7.3	58		92
	7425	2.5	0.3	1670	255		18	7.3	51		103
	8621	2.8	0.3	1580	270		40	7.3	38	63	139
H_2	18	2.8	72		7		134	7.3	15	67	197
4.0 K	25	3.1	70	147	8		338	7.0	2.3	110	198
	46	3.1	66	100	9		452	7.3	2.1	115	227
	159	3.1	49	95	18		724	8.4	2.1	110	268
	1232	2.5	2.9	185	22		1228	9.2	2.1	103	343
	1789	2.0	0.7	125	38	T_2	4	6.4	55		53
	2698	1.7	0.3	141	42	6.3 K	10	6.4	53	108	65
	3137	1.7	0.3	200	41		31	6.4	37	121	80
	4317	1.4	0.3	436	34		150	6.2	12		119
	8647		0.3	1170			236	5.9	3.6	140	121
	9904		0.3	2500	39		494	5.6	2.2	166	150
H_2	2	3.4	75		14		617	5.9	2.2	130	157
5.4 K	8	3.4	74	45	24		892	6.2	2.2	133	173
	24	3.6	70	39	31		1263	6.4	2.2	150	191
	92	3.9	58	36	29	T_2	7	6.4	59		34
	4397	1.1	0.3		13	8.1 K	560	4.2	2.9	167	63
	5776	0.8	0.3	4350	13		764	4.5	2.9		67
	7245	1.1	0.3		14		1201	4.5	2.9	171	76
	8866	1.1	0.3		17	T_2	1	10.4	68		17
T_2	36	12.7	51	56	1045	10.1 K	16	8.4	43		20
2.2 K	57	15.4	48		1406		42	5.6	21		22
	79	16.9	45		1685		92	3.4	7.9	84	27
T_2	11	9.1	65	43	130		152	3.4	5.3	99	37
2.1–2.3 K	47	11.7	58	42	480		335	3.4	4.9	100	39
	63	12.6	55	40	554		534	3.4	4.9	104	42
T_2	31	5.3	53		44		734	3.6	4.9		51
4.0 K	48	7.3	48	13	160		1083	3.9	4.9	144	74
	65	7.6	40	20	180						

TABLE II. Measured relaxation times, $J=1$ compositions, and atom densities for solid HD, D_2, and D-T.

Hydrogen	Time (min)	Linewidth (MHz) H in HD	Linewidth (MHz) D in HD	Electron T_{1e} (ms) H in HD	Electron T_{1e} (ms) D in HD	Total atoms (ppm)
HD	6	9.4	7.5			39
1.3 K	28	8.8	8.6			47
	47	9.8	10.1	640	640	83
	85	10.2	9.8	590	620	139
	156	10.8	11.1	610	630	208
HD	18	8.7	9.2			27
2.4 K	48	9.2	9.2			63
	128	9.5	10.6	603	541	104
	1045	10.1	10.6	353	520	147
	1452	10.1	10.4	305	500	243
	2416	10.4	10.4	302	395	255
	5368	10.4	9.2	200	315	307
HD	245	9.0	9.5			93
3.4 K	923	9.8	10.4			106
	1606	11.8				224
	2544	11.5	12.1			223
	Time	Linewidth (MHz)		Electron T_{1e} (ms)		Atoms
Hydrogen	(min)	Middle	High	Middle	High	(ppm)
D_2	12	9.3	5.0			42
1.4 K	33	9.3	6.0			72
	62	9.8	6.2			140
	130	9.3				193
	936	11.5	10.6	81	70	590
	1390	12.3	12.0		62	685
D_2	37	5.8	6.1			26
4.2 K	360	6.0				84
	969	6.1	5.5			72
	3055	6.4	6.3			96
	4428	6.1	4.4			126
	5769	7.0	6.8		120	110
	7353	7.4	6.8			133
	8548	7.1	6.8	157	149	148
	9909	7.2	6.5			172
		D in D-T	T in D-T	D in D-T	T in D-T	
D-T	6	10.4	9.2	144	145	145
3.0 K	40	9.2	12.1	110	283	283
	211	11.8	12.3			399
	295	11.8	12.1	70	423	423
	360	11.8	12.1	81	433	433
	536	11.8	12.1	84	426	426
	1219	11.8	13.2	88	451	451
D-T	11	10.1	10.6	143	104	104
4.0 K	26	10.9	10.6			128
	51	10.6	10.6	107	154	154
	107	10.6	10.6			210
	163	11.2	10.4	95	265	265
	217	11.2	11.8	104	290	290
	1006	11.2	12.1	114	307	307
	1400	10.4	12.1	116	210	360
D-T	7	8.4	9.2			105
5.1 K	37	8.7	9.0			125
	74	8.4	9.0	159	155	155
	199	9.2	9.2	138	168	168
	376	10.4	10.4	154	211	211
	1046	10.4	11.2	181	245	245

TABLE II. (*Continued*).

Hydrogen	Time (min)	Linewidth (MHz) D in D-T	Linewidth (MHz) T in D-T	Electron T_{1e} (ms) D in D-T	Electron T_{1e} (ms) T in D-T	Total Atoms (ppm)
D-T	59	11.2	9.8	153	40	40
6.3 K	131	9.2	9.2	161	64	64
	425	10.4	9.5	164	102	102
	1130	10.6	11.8	198	124	124
	2467	11.2	12.1	205	174	174

The T_{1e}'s measured in these experiments ranged from 20 ms to 5 s. All of our samples showed exponential T_{1e} curves.

III. RESULTS

We first present the ESR spin-lattice relaxation data, taken on five solid hydrogens. In Table I, we list the measurements taken on H_2 and T_2, both with only a single NMR-active $J=1$ state and a single kind of atom to measure. We measured the upper hyperfine line in all cases. These hydrogens can have the $J=1$ species decline to small vales. In Table II we list the hydrogens that always possess a NMR-active species: HD, D_2, and D-T. For HD, the $J=1$ concentration is unknown but small. We measured the upper hyperfine atom line for H and T and generally the high hyperfine line for D. In D_2, we measured the middle hyperfine line as well. All data presented here were taken without the known presence of thermal spikes, which would add a further complication.

We next turn to the lines shapes, as defined by Eqs. (1)–(3). The best data were obtained with solid H_2 and T_2, which each have only the single nuclear magnetic $J=1$ species. These data are shown in Fig. 1, where time runs from right to left. The 2–6 K T_2 region is well represented by the 5-K T_2 data, where the line shape is close to Gaussian only at the start of the experiment, where the $J=1$ T_2 concentration is about 70%. As the $J=1$ T_2 concentration decreases by conversion, the line shape quickly changes to Lorentzian. The process is slightly more gradual for T_2 at 8 K and H_2 from 1.4 to 5.4 K. T_2 at 10 K remains near Gaussian longer and changes shape at much lower $J=1$ T_2 concentrations. The line-shape determinations have much more scatter for the other hydrogens. The fraction of the Lorentzian component was found to be H in HD, 0.5 ± 0.3; D in HD, 0.5 ± 0.4; D in D_2, 0.7 ± 0.3; D in D-T, 0.7 ± 0.3; and T in D-T, 0.6 ± 0.3 for all temperatures, varying from 1.4 to 5.4 K. For high-field D_2, a single Gaussian line shape was found at the very start. All other D_2 lines averaged to 0.8 ± 0.2. Most line shapes are definitely not Gaussian.

Sharnoff and Pound believed that their ESR lines were homogeneous (at least for a 6-MHz width), because they could not burn a hole in the line.[3] We also could not, but we feel the presence of non-Gaussian lines is an indication that the longer-time ESR lines may be inhomogeneous. Figure 2 shows the result of a special measurement, taken on solid T_2 at 4.0 K. The sample was 1150 min old, contained 370 ppm atoms and possessed a line width of 9.6 MHz. The line center T_{1e} measurement by saturation recovery gave a value of 69 ms. The 9.4-GHz microwave source was narrow banded compared to the linewidth. We measured T_{1e} as a function of position on the ESR line, and we find that, for this sample, T_{1e} is a function of position. We take this as further evidence that some ESR lines could be inhomogeneous.

All data in this paper have been chosen not to include known thermal spikes. Unfortunately, the only data that suggest the possible presence of hidden atoms occur in spiking samples, as shown in Fig. 3. The source is pure T_2 at 2.2 K kept to long times at 1.7–2.5 K, with considerable jitter in the temperature. At long times, the atom signal declines but the linewidth stays constant, suggesting that atoms have moved so close to one another that the linewidth has broadened out of sight. Thermal spikes occurred in the sample from 80 min on, with a confirmed atom concentration decrease caused by a temperature surge to 3.3 K at 2770 min. We have since optically viewed solid D-T undergoing thermal spiking and discovered that the process has the ability to blow the sample around in its cryogenic cell. Thus the decline in

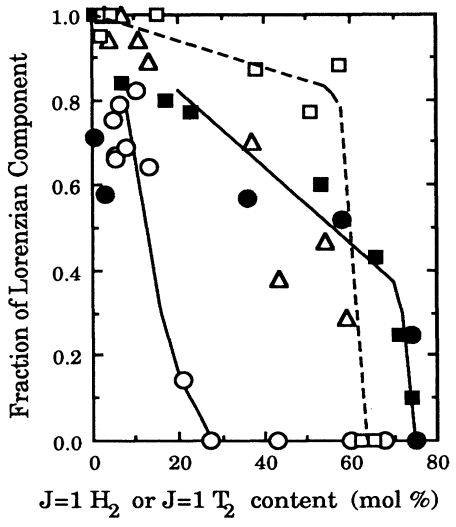

FIG. 1. Fraction of Lorentzian line shape as a function of $J=1$ hydrogen for solid H_2 and T_2 samples. Time runs from right to left. The line shapes are closest to Gaussian only for $J=1$ values near 75% and change quickly toward the Lorentzian shape. The samples are H_2 1.4 K (■); 5.4 K (●); T_2 5.1 K (□); 8.1 K (△); and 10.1 K (○).

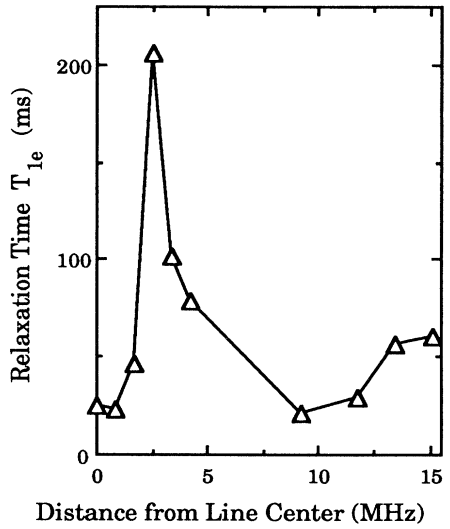

FIG. 2. Longitudinal relaxation time for the hydrogen atom in solid T_2 at 4.0 K as a function of the distance from the line center. A narrow-band microwave source was used. This offers evidence that this ESR line is inhomogeneous.

signal in Fig. 3 could be caused by the sample being removed from the ESR measurement region. It appears that the hidden atom question must be solved in solid hydrogens with little or no tritium.

IV. THE ESR LINEWIDTH CALCULATION

We have mentioned that even the mechanism of line broadening is in dispute at this time. Miyazaki *et al.*[4,5]

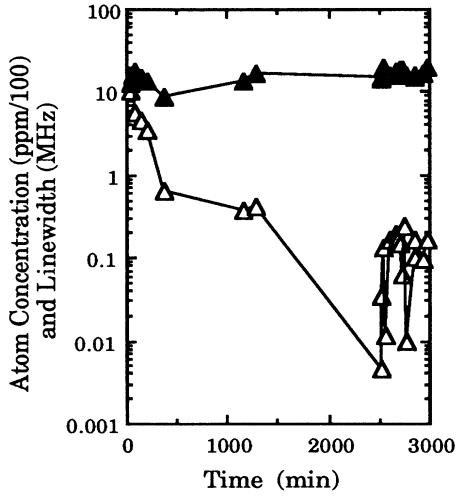

FIG. 3. Possible evidence for "hidden" hydrogen atoms: atom concentrations [ppm, divided by 100 (△)] and measured linewidths in MHz (▲) in a solid T_2 sample kept at 1.7–2.5 K for a long time. The atom concentraton declines dramatically but the linewidth stays constant. Heat spikes occurred in the sample from 80 min on and may have blown the sample out of the measurement volume. Over 1000 ppm atoms were present in the T_2 at early times.

have proposed the hyperfine interaction that is the dominant line broadening mechanism for F centers in irradiated alkali halides. This has been treated theoretically by Kip *et al.*,[10] and the dominant interaction Hamiltonian for F centers can be written, in Système International (SI) metric units, as

$$H=\sum_i \frac{\mu_0}{4\pi}\left[\frac{h^2\nu_e^0\nu_{ni}^0}{3I_i}|\Psi_i|^2\right]\mathbf{I}_i\cdot\mathbf{S}\ , \tag{5}$$

where $\mu_0/4\pi=10^{-7}$ N/A^2, h is Planck's constant, ν_e^0 and ν_{ni}^0 are the magnetic resonance frequencies in MHz/T of the electron and of the nuclei of the neighboring molecule, $|\Psi_i|^2$ is the properly orthogonalized overlap integral of the atomic wave function at the site of the ith neighboring molecule, $\mathbf{I}_i$ is the nuclear spin of the ith neighboring molecule, and $\mathbf{S}$ is the spin of the electron. The nuclear spin can take on $2I+1$ values. For n nearest neighbors, there are $(2I+1)^n$ values of the total nuclear spin component parallel to the externally applied magnetic field (M_I). This distribution of M_I gives rise to a Gaussian line shape with a second moment

$$M_2^{\rm hyp}=\left[\frac{\mu_0 h\nu_e^0}{4\pi}\right]^2\frac{16\pi^2}{27}\sum_i(\nu_{ni}^0)^2\frac{I_i+1}{I_i}|\Psi_i|^4\ . \tag{6}$$

It is difficult to calculate $M_2^{\rm hyp}$ theoretically because calculating $|\Psi_i|^2$ requires the nearest-neighbor distance between the atomic impurity and the neighboring molecules in the lattice. On the other hand, if the hyperfine interaction is the dominant broadening mechanism, we can use Eq. (6) to determine $|\Psi_i|^2$.

The F center is an electron with no nucleus to localize it, whereas this is not the case for a hydrogen atom. The interaction potential between a hydrogen atom and a hydrogen molecule has a strong hard core at close distances. Thus an atom in a hydrogen lattice causes severe lattice distortions in the immediate vicinity of the atom. Danielowicz and Etters have calculated that a H atom is bound at a lattice site in solid H_2 in a well 15.9 K deep and the intermolecular distance swells from 0.378 nm by 6% in the first shell.[11] Cao and Gaines have since calculated the lattice distortion for an atom in both the interstitial positions in solid H_2.[12] They found that the nearest neighbor in the larger interstitial position moved from 0.27 to 0.355 nm and the smaller interstitial distance increased from 0.23 to 0.32 nm. These huge effects would tend to further decouple the atom from overlapping nearby nuclei.

Moreover, if the atom were sitting within 0.2 nm of a neighboring molecule, a large effect would be seen in the hyperfine splitting and the g factor. The Pauli exclusion interaction should tend to pinch the atom's electronic wave function onto its nucleus, increasing the hyperfine splitting. The exclusion interaction would also cause a small mixing of the p orbital into the ground atomic s state, thus allowing a shift in the g factor. Adrian has estimated that a H atom at a distance of about 0.23 nm would cause more than a 1% shift in the hyperfine splitting.[13] Previous measurements show that the hyperfine coupling constant A and the shift in the g factor are very

close to the free atomic value. Previously measured deviations in the hyperfine coupling, $[A - A(\text{free})]/A(\text{free})$, for H, D, or T atoms in H_2, D_2, or T_2, vary from 0.1% to 0.3%.[14]

For these reasons, we turned to the weak dipolar approach. Kittel and Abrahams have considered the dipolar broadening of magnetic lines caused by the interaction of electrons randomly spaced on a crystal lattice.[15] They conclude that for concentrations of electron spins over 10%, the line shape will be Gaussian and the linewidth (proportional to the square root of the second moment) will change with the half power of the spin concentration. Also, for spin concentrations below 1%, the line shapes will be Lorentzian and the linewidth will change as the first power of the electron concentration. For the Lorentzian line shape, the second moment cannot be defined.

For a Gaussian line, the full linewidth at half height, $\Delta\nu$, is related to the total second moment M, by the relation[8]

$$\Delta\nu = 2.36 M^{1/2} , \tag{7}$$

where all the components of the total second moment are expected to be additive.

We begin with the nuclear-electron contribution to the second moment, the starting point used by Sharnoff and Pound.[3] We must consider the Hamiltonian H for a pair of dipoles, which is often presented in this form as described by Slichter:[16]

$$H = \left[\frac{\mu_0}{4\pi}\right][A+B+C+D+E+F]\frac{h^2\nu_e^0\nu_n^0}{R_0^3} , \tag{8}$$

where R_0 is the intermolecular distance between the dipoles. Terms C–F all require energy exchange between the dipoles and so do not affect the linewidth. The A term describes the z component of the spins; it contains all diagonal matrix elements and induces no spin flips. The B term is operative when there is spin flipping between the two magnetic moments. If the ESR and NMR energies were the same, then both the A and B terms would be included in the second moment. But the resonance frequencies are different, and the B term drops out of the calculation. The resulting second moment is $\frac{4}{9}$ the size of the equal-energy result. Then, the rigid lattice nuclear second moment with all sites filled, $M_n(\infty)$, becomes

$$M_n(\infty) = \left[\frac{\mu_0}{4\pi}\right]^2 \frac{4}{9}\frac{h^2(\nu_e^0)^2(\nu_n^0)^2}{R_0^6}\frac{3}{5}14.455\alpha I(I+1) , \tag{9}$$

where α is a lattice distortion parameter. For the nuclei H, D, and T, the NMR frequencies ν_n^0 are 42.576, 6.536, and 45.413 MHz at 1 T, respectively. The infinity sign indicates that all lattice sites are occupied by the nuclear spin I and that the atom is itself on a lattice site. The "$\frac{3}{5}$" indicates a powder average over small randomly oriented crystallites. The lattice sum is calculated from the jth electron spin to the k nuclear spins around it on every lattice site.[16] For a hexagonal close-packed structure, this number in units of R_0^6 is 14.455, as shown in Eq. (9).[17,18] The final second moment is the sum of terms from all nuclear species:

$$M_n = 0.01\sum_i [J]_i\alpha_i(J)M_n(\infty)_i , \tag{10}$$

where we sum across the i pure nuclear magnetic species with nonzero nuclear spin of varying mol %, $[J]_i$. A single term suffices for H_2 and T_2 but a set of terms is needed for the other hydrogens.

We turn to the electron-electron linewidth interaction, where the rigid dipole approach above produces linewidths that are far too broad. Instead, a dilute-spin theory is needed, and this has been recently reconsidered by Drabold and Fedders.[19] They considered 11 magnetic dipoles in a random lattice and solved exactly the energy levels created by the weak dipolar interaction, which created a homogeneous ESR line. Then, the interaction of each spin with its nearest neighbors was calculated. If these interactions lay outside the homogeneous energy band, they created an inhomogeneous linewidth and those spin interactions were removed from the homogeneous energy band, which shrank to a narrower size. This process was repeated until the solution converged with 30% homogeneous spins in a central Gaussian-like structure and 70% inhomogeneous spins in a broader Lorentzian-like structure. The center half of the resulting line is homogeneous and the outer half inhomogeneous, where each inhomogeneous "slice" is only one spin wide. If the time for a spin to diffuse across the homogeneous center is the transverse relaxation time T_2, then the time across the inhomogeneous portion is perhaps $100T_2$. The result is independent of the crystal structure if the spin concentration is dilute. A series of numerical computer models were run and the solutions summarized. The ESR linewidth, including both homogeneous and inhomogeneous components, is

$$\Delta\nu_e = \left[\frac{\mu_0}{4\pi}\right]1.046\times10^{-5}[\text{atom}]\frac{h(\nu_e^0)^2}{R_0^3} , \tag{11}$$

where [atom] is the atom conventration in ppm. We note that the similar statistical theory of Abragram has the coefficient 1.074×10^{-5} in Eq. (11),[20] while the earlier Kittel-Abrahams result was 1.50×10^{-5}.[15] As an example, Eq. (11) predicts a linewidth of 1.2 MHz for 100 ppm of atoms in pure tritium.

The undistorted intermolecular distances for H_2, HD, D_2, DT, and T_2 are taken to be 0.3784, 0.3688, 0.3603, 0.3564, and 0.3534 nm, respectively.[21]

V. DISCUSSION

Our approach has focused on seeking clear-cut atom-$J=1$ nuclear or atom-atom interactions in our samples. Figure 4 illustrates the problem with H_2 at 1.4 K. The near-constant linewidth is analyzed in terms of a strong $J=1$ interaction at early times and a strong atom-atom interaction at long times. Unfortunately, H_2 is unique in dropping to negligible $J=1$ concentrations, whereas most

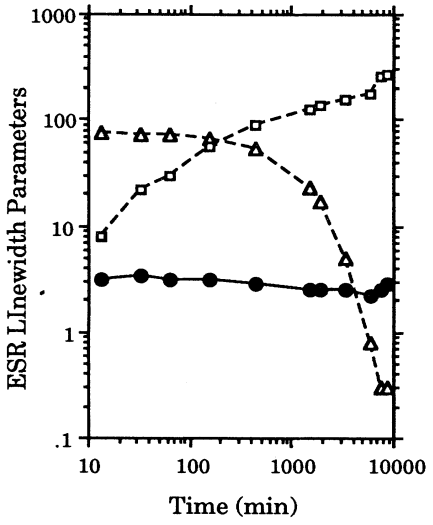

FIG. 4. Linewidth parameters for H_2 at 1.4 K, illustrating how the atom concentration (in ppm, □) and $J=1$ H_2 concentration (%, △) are thought to sum to the measured linewidth (MHz, ●). Unfortunately, this is one of a few samples to so clearly show this effect.

of our samples contain $J=1$ spins in abundance.

We turn first to the linewidth calculations. The results of Miyazaki's linewidth calculations are listed in Table III. He obtains agreement for H_2 with the atom on an empty lattice site, but the calculated linewidths for HD and D_2 are too small. He is able to obtain agreement by moving the atom to an interstitial site, with the assumption that the crystal remain undistorted.

Table III also lists the results of our weak dipolar calculations for the nuclear-electron interaction, which we expect to be dominant for high $J=1$ concentrations with a small atom presence. All calculations assume the atoms to be on an undistorted lattice site from which a molecule is missing. The calculated linewidths are just right for HD and T_2 only at 10.4 K, but are somewhat too broad for all the rest of the T_2 data and the D-T results. The calculated values are far too broad for both H_2 and D_2. This effect for H_2 has been noticed before by several researchers[4,5,14,22,23] and an old suggestion is that the nearest-neighbor $J=1$ H_2 molecules have been converted to $J=0$ by the catalytic presence of the atom.[22,23] Removing this shell reduces the calculated linewidth to 3.4 MHz, in agreement with the measurement.

The probable truth is that neither pure Gaussian theory can be expected to work for more than a handful of data points, because other mechanisms convert the line shape toward the Lorentzian.

We next consider the electron-electron interaction, which we expect to add 1 MHz of linewidth for every 100 ppm atoms. Again, we can look to only a handful of possible pure cases; i.e., those for H_2 and T_2 where the $J=1$ concentration has been reduced to a small number and the atom concentration is above 150 ppm. We find 1.1 MHz/(100 ppm) atoms for H_2 at 1.4 K and 3.4 MHz/(100 ppm) in T_2 at 4.0–6.3 K. Here, too, we are not able to isolate results in good agreement with theory.

Our major problem is that nuclear magnetic and atom effects are present at the same time in virtually all samples. We find empirically that reasonably good agreement, as shown in Fig. 5, is obtained by plotting linewidth as a function of the parameter Q, which is defined by

$$Q=0.030\nu_n^0[I(I+1)]^{1/2}[J=1]^{1/2}+[\text{atom}]^{1/2}\ . \qquad (12)$$

TABLE III. Comparison of calcualted Gaussian linewidths with measured linewidths with near-normal solid hydrogens containing minimum concentrations of hydrogen atoms. Miyazaki's calcualtions assume wave-function overlap, whereas our assume the weak dipolar interaction. Only the true Gaussian lines may be legitimately compared with the calculations.

			ESR linewidth (MHz)		
Source	Hydrogen	Temp. (K)	Measured	Calc. lattice site	Calc. large interstitial site
Miyazaki	H_2	4.2	1.0	0.7	11.8
	HD	4.2	7.3	0.5	8.4
	D_2	4.2	3.4	0.2	3.1
Gaussians, our results	H_2	1.4	3.2	8.0	
		4.0	3.0	8.0	
		5.4	3.5	8.0	
	D_2	4.2	6.0	2.3	
	T_2	10.4	10.4	10.5	
Not Gaussian, our results	HD	1.3–3.4	8–9	9.5	
	D_2	1.4,4.2	5–9	2.3	
	*n*D-T	3.0–6.3	8–11	7.7	

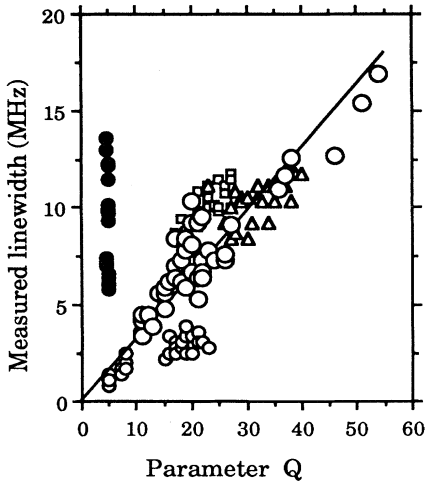

FIG. 5. The best overall linewidth description in a plot of the measured ESR linewidths as a function of the empirical parameter Q which combines both nuclear and atom effects. The points are H_2 (○); H in HD (□); D_2 (●); D in D-T (△); and T_2 (○). The 1.4-K H_2 points are slightly low, and the D_2 data totally fail to fit into this framework.

This is a combination of strong half-power interactions of both nuclei and atoms, with the coefficient being empirically determined. In HD and D-T, the H and T nuclei will dominate this parameter. Most of the data fit reasonably well on this plot, with the H_2 points at 1.4 K being slightly low and the true Gaussian 10.4 K T_2 point being slightly high. Completely off are all the D_2 data, which remain broad despite the weakness of the deuteron magnetic moment. The broadening occurs if nuclear spins are present, regardless of their strength.

We now briefly comment on the electron's longitudinal relaxation time T_{1e}. The most noticeable feature is how constant T_{1e} is, remaining between 0.1 and 1s. An exception occurs for H_2 with small $J=1$ concentrations; this was also noticed by Iskovskikh *et al.*[24] We suggest that the *EQQ* mechanism is present at these low concentrations. Drabold and Fedders derived an *EQQ* nuclear relaxation equation for protons in solid HD at low $J=1$ concentrations, i.e., below the T_{11} minimum.[25] It is

$$T_{11}=3.1\times10^{-15}\nu_n^{8/5}/[J=1\ \mathrm{H_2}]^{3/2}T^{7/5}\ , \tag{13}$$

where T is the temperature. The denominator contains the interaction frequency ν_j, which is

$$\nu_j=\left[\frac{\mu_0}{4\pi}\right]\frac{h\nu_0^0\nu_J^0 IJ}{r^3}\ , \tag{14}$$

where ν_J^0 is the $J=1$ hydrogen rotational frequency of 6.73 MHz/T, and r is the distance between the nuclei and the rotational moment. A similar equation may be written for the electron. The resonance frequencies are 42.6 and 28 025 MHz/T for the nuclear and electronic cases, but the distances are about 0.074 and 0.40 nm, respectively. This leads to ν_J values of about 47 and 97 kHz, respectively; i.e., the constants are about the same. For the electron, we have

$$T_{1e}=7.3\times10^{-16}\nu_e^{8/5}/[J=1\ \mathrm{H_2}]^{3/2}T^{7/5}\ . \tag{15}$$

We find that Eq. (15) indeed delivers a few seconds for our H_2 samples at the lowest $J=1$ values, in agreement with the data. It appears, however, that all other samples have relaxation determined by a mix of $J=1$ concentration and atom density.

We conclude by noting that the relaxation properties of the visible atoms are not explained by simple relationships of the $J=1$ or atom concentrations, so that the effect of hidden atoms is indeed a possibility.

ACKNOWLEDGMENTS

We would like to thank Chris Gatrousis and Tom Sugihara of the Chemistry and Materials Science Department and John Holzrichter and John Nuckolls of the Institutional Research and Development fund for their support of this work. This work was performed under the auspices of the U.S. Department of Energy by the Lawrence Livermore National Laboratory under Contract Number W-7405-ENG-48.

[1]G. W. Collins, P. C. Souers, J. L. Maienschein, E. R. Mapoles, and J. R. Gaines, Phys. Rev. B **45**, 549 (1992).
[2]J. R. Gaines, Y. Cao, and P. A. Fedders (unpublished).
[3]M. Sharnoff and R. V. Pound, Phys. Rev. **132**, 1003 (1962).
[4]T. Miyazaki, Chem. Phys. Lett. **176**, 99 (1991).
[5]T. Miyazaki, H. Morikita, K. Fueki, and T. Hiraku, Chem. Phys. Lett. **182**, 35 (1991).
[6]G. W. Collins, E. M. Fearon, J. L. Maienschein, E. R. Mapoles, R. T. Tsugawa, P. C. Souers, and J. R. Gaines, Phys. Rev. Lett. **65**, 444 (1990).
[7]G. W. Collins, E. M. Fearon, E. R. Mapoles, R. T. Tsugawa, P. C. Souers, and P. A. Fedders, Phys. Rev. B **44**, 6598 (1991).
[8]A. Abragram, *The Principles of Nuclear Magnetism* (Clarendon, Oxford, 1961), pp. 106–108.
[9]C. F. Davis, Jr., M. W. P. Strandberg, and R. L. Kyhl, Phys. Rev. **111**, 1268 (1958).
[10]A. F. Kip, C. Kittel, R. A. Levy, and A. M. Portis, Phys. Rev. **91**, 1066 (1953).
[11]R. L. Danielowicz and R. D. Etters, Phys. Rev. B **19**, 2321 (1979).
[12]Y. Cao and J. R. Gaines (private communication).
[13]F. J. Adrian, J. Chem. Phys. **32**, 972 (1959).
[14]C. K. Jen, S. N. Foner, E. L. Cochran, and V. A. Bowers, Phys. Rev. **112**, 1169 (1958).
[15]C. Kittel and E. Abrahams, Phys. Rev. **90**, 238 (1953).
[16]C. P. Slichter, *Principles of Magnetic Resonance* (Harper & Row, New York, 1963), pp. 50–59.
[17]J. Van Kranendonk, *Solid Hydrogen* (Plenum, New York, 1983), pp. 295–296.
[18]T. Kihara and S. Koba, J. Phys. Soc. Jpn. **7**, 348 (1952).
[19]D. A. Drabold and P. A. Fedders, Phys. Rev. B **37** 3440 (1988).
[20]A. Abragram, *The Principles of Nuclear Magnetism*, Ref. 8, pp. 125–128.
[21]P. C. Souers, *Hydrogen Properties for Fusion Energy* (University of California, Berkeley, 1986), pp. 78–80.
[22]J. C. Solem and G. A. Rebka, Phys. Rev. Lett. **21**, 19 (1968).
[23]A. S. Iskovskikh, A. Ya. Katunin, I. I. Lukashevich, V. V. Sklyarevskii, and V. A. Shevtsov, Pis'ma Zh. Eksp. Teor. Fiz. **42**, 26 (1985) [JETP Lett. **42**, 30 (1985)].
[24]A. S. Iskovskikh, A. Ya. Katunin, I. I. Lukashevich, V. V. Sklyarevskii, V. V. Suraev, V. V. Filippov, N. I. Filippov, and V. A. Shevtsov, Zh. Eksp. Teor. Fiz. **91**, 1832 (1986) [Sov. Phys. JETP **64**, 1085 (1986)].
[25]D. A. Drabold and P. A. Fedders, Phys. Rev. B **39**, 6325 (1989).